

## Anisotropic diffuse x-ray scattering in early transition metal oxide structures

This article has been downloaded from IOPscience. Please scroll down to see the full text article.

2007 J. Phys.: Condens. Matter 19 275208

(<http://iopscience.iop.org/0953-8984/19/27/275208>)

View [the table of contents for this issue](#), or go to the [journal homepage](#) for more

Download details:

IP Address: 129.252.86.83

The article was downloaded on 28/05/2010 at 19:38

Please note that [terms and conditions apply](#).

# Anisotropic diffuse x-ray scattering in early transition metal oxide structures

**T Malcherek**

Mineralogisch-Petrographisches Institut, Universität Hamburg, Grindelallee 48,  
D-20146 Hamburg, Germany

E-mail: [thomas.malcherek@uni-hamburg.de](mailto:thomas.malcherek@uni-hamburg.de)

Received 4 January 2007, in final form 29 January 2007

Published 1 June 2007

Online at [stacks.iop.org/JPhysCM/19/275208](http://stacks.iop.org/JPhysCM/19/275208)

## Abstract

Occurrences of strongly anisotropic diffuse scattering in planes of reciprocal space are reported for early transition metal oxides of the titanite and pyrochlore structure types. The diffuse scattering sheets are compared to corresponding observations in  $\text{KNbO}_3$  and  $\text{BaTiO}_3$ . Possible structural models are discussed in relation to existing models of the diffuse scattering effects in these perovskite ferroelectrics.

(Some figures in this article are in colour only in the electronic version)

## 1. Introduction

Early transition metal oxides constitute an important part of those ferroics with interesting and technically important physical properties. The electronic configuration of early transition metal cations (e.g.  $\text{M} = \text{Ti}^{4+}$ ,  $\text{Nb}^{5+}$ ,  $\text{V}^{5+}$  or  $\text{Mo}^{6+}$ ), which is commonly  $d^0$  or  $d^1$ , gives rise to distorted  $\text{MO}_6$  oxygen octahedra, provided the size and charge of the cations favour such a distortion (Kunz and Brown 1995, Brown 2002). As a result non-centric chemical bonds occur towards the oxygen ligands. Even if such distortions are symmetry-forbidden for the average structure, they might still occur locally. Distinctive anisotropic diffuse scattering may then arise if the local distortions correlate among certain, structurally favourable directions. However, these correlations need not necessarily arise from static disorder. If the dispersion relation of low frequency phonons has a strong directional dependence, dynamic correlations may give rise to similarly anisotropic diffuse scattering effects (Hüller 1969).

Diffuse scattering is usually several orders of magnitude weaker than the Bragg scattering. In order to observe it either a very long exposure time or very intense incident radiation is required. Therefore observation of these diffuse scattering effects is achieved most effectively by single crystal synchrotron-x-ray or electron diffraction experiments.

The aim of this paper is to compare the occurrence of extended diffuse scattering sheets in several oxide compounds of early transition metals. So far perovskite structures have attracted

the most attention in this respect. The other more complex oxide compounds presented here are chemically and structurally similar to the perovskites in so far as they also contain early transition metal cations M (= Ti, Nb or Ta) in octahedral coordination. The recurring feature common to all relevant structures appears to involve chains of trans-corner-connected  $\text{MO}_6$  octahedra. Topologically, such chains may be isolated or they may cross to form three-dimensional networks. The chains may also be subject to varying degree of distortion induced by the other structural building blocks.

### 1.1. Perovskite ferroelectrics

A well known example of strongly anisotropic diffuse scattering is that located along reciprocal lattice planes (relplanes) normal to  $\langle 100 \rangle$  in the perovskite ferroelectrics  $\text{KNbO}_3$  and  $\text{BaTiO}_3$ . Ever since Comes *et al* (1968) observed and interpreted these diffuse sheets, the exact origin of the phenomenon has been a matter of debate. In accordance with the sequence of phase transitions of  $\text{KNbO}_3$  from cubic to tetragonal to orthorhombic to rhombohedral, the three equivalent sets of diffuse sheets seen in the cubic phase reduce to only two in the tetragonal phase and just one in the orthorhombic phase (Comès *et al* 1970). No diffuse scattering sheets are observable in the low temperature rhombohedral phase and generally no diffuse scattering is visible on relplanes that pass through the origin (Comes *et al* 1968). Early theories favoured the explanation by a purely displacive model (Hüller 1969). This involves linear chains of correlated displacements in the transverse optical zone centre soft mode. The alternative model of static eight-site order–disorder (Bersuker 1966, Chaves *et al* 1976) was invoked by Comes *et al* to explain the diffuse scattering sheets. Mainly because of the large Curie–Weiss constant observed in perovskite ferroelectrics, such an order–disorder behaviour of perovskite ferroelectrics was deemed unlikely at the time. However, more recent x-ray absorption measurements (Mathan *et al* 1993, Ravel *et al* 1998) confirmed that Nb and Ti in the cubic phases of  $\text{KNbO}_3$  and  $\text{BaTiO}_3$  are not located at their nominal high symmetry site but close to those sites predicted by the Comes model, i.e. displaced along  $\langle 111 \rangle$  towards the octahedral face centres. Experimental and computational results suggest that perovskite ferroelectrics simultaneously display displacive and order–disorder properties (Girshberg and Yacoby 1997). According to Girshberg and Yacoby (1999), the off-centre displacements at different sites are coupled via the soft-mode, leading to a ferroelectric phase transition. The Ti displacements have recently been verified by the observation of non-zero quadrupolar coupling of  $^{47,49}\text{Ti}$  in single crystal NMR experiments on  $\text{BaTiO}_3$  (Zalar *et al* 2003, 2005). Yu and Krakauer (1995) have studied the ferroelectric phase transitions in  $\text{KNbO}_3$  by first-principles calculations and found that the unstable mode is associated with infinite chains of coherently displaced Nb atoms, while shorter chains or individually displaced Nb atoms would not be unstable. These chain-displacements appear to be dynamic rather than static (Krakauer *et al* 1999). Chapman *et al* (2005) measured thermal diffuse scattering in the cubic paraphase of  $\text{PbTiO}_3$  and did not observe any two-dimensional diffuse scattering effects similar to  $\text{BaTiO}_3$  or  $\text{KNbO}_3$ .  $\text{PbTiO}_3$  not only has the highest ferroelectric transition temperature of the perovskite ferroelectrics (at 763 K), but also remains tetragonal down to low temperatures, with a large tetragonal strain compared to  $\text{BaTiO}_3$ , for example. Local displacements of both Pb and Ti persist well into the cubic phase of  $\text{PbTiO}_3$  (Sicron *et al* 1994). However, the direction of these displacements is not consistent with the eight-site model, as they are directed along  $\langle 001 \rangle$  instead of  $\langle 111 \rangle$ . In contrast to  $\text{PbTiO}_3$ , diffuse scattering on relplanes normal to  $\langle 100 \rangle$  has been observed in the incipient ferroelectric  $\text{KTaO}_3$ , where it has been found to be largely in agreement with the dynamic model of Hüller (1969) (Comès and Shirane 1972). The effect is not restricted to zone-centre instabilities either, as the example of anisotropic diffuse scattering in  $\text{NaNbO}_3$  demonstrates (Denoyer *et al* 1971).

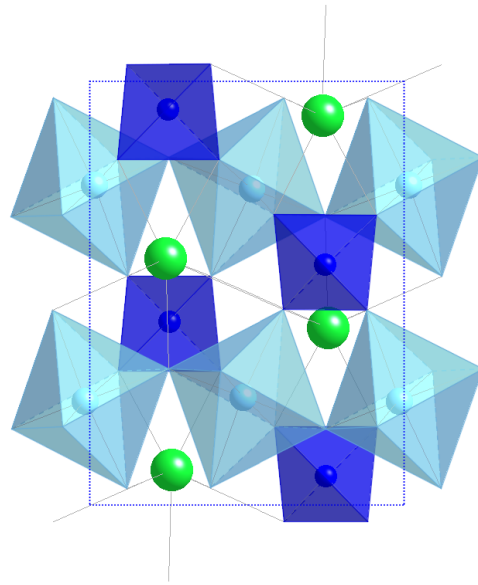


**Figure 1.** The structure of the low temperature form of titanite. The oxygen atoms at the corners of the polyhedra are not shown.

Because Pb itself hybridizes with the oxygen atoms in  $\text{PbTiO}_3$ , the tetragonal ground state is stabilized over the rhombohedral ground state via strain coupling (Rabe and Waghmare 1997) in this case. In the cubic paraphase local tetragonal strains suppress the formation of correlated  $\langle 001 \rangle$  Ti displacements (Chapman *et al* 2005). In  $\text{BaTiO}_3$ , on the other hand, ‘tetragonal nanodomains’, tantamount to a tetragonally distorted eight-site model, have been shown to possess finite lifetime in the cubic paraphase of  $\text{BaTiO}_3$ , while the lattice, i.e. the Ba–O framework, remains cubic (Zalar *et al* 2005). The dynamic exchange of these nanodomains is at least two orders of magnitude slower than the ‘rattling’ of the Ti-cations within their eight-site cage. Such a picture of dynamic nanodomains is in agreement with the computational results obtained by Yu and Krakauer (1995) and Krakauer *et al* (1999), predicting dynamic chain-like correlations of the Ti displacements in  $\text{KNbO}_3$ .

## 2. The titanite structures

The mineral titanite (or *sphene*) has the idealized stoichiometry  $\text{CaTiOSiO}_4$ . The titanite structure is formed by lateral connection of parallel chains of trans-corner-sharing  $\text{TiO}_6$  octahedra via isolated  $\text{SiO}_4$  tetrahedra. The resulting framework is charge balanced by seven-coordinated Ca, which is located on the direct line between Si and the O1 atom. O1 is the corner-sharing atom of the octahedral chains (figure 1). In this type of structure the three-dimensional network of corner-sharing  $\text{MO}_6$  octahedra of the perovskites is replaced by a parallel arrangement of one-dimensional chains of such octahedra, distended by the  $\text{XO}_4$  tetrahedra.

The Ca position of titanite may be occupied by other alkaline earth or alkaline metals. It might also be vacant, depending on the charge of the titanite framework. Many derivatives of the titanite structure of stoichiometry  $\text{AMOXO}_4$  are known, with space group symmetries

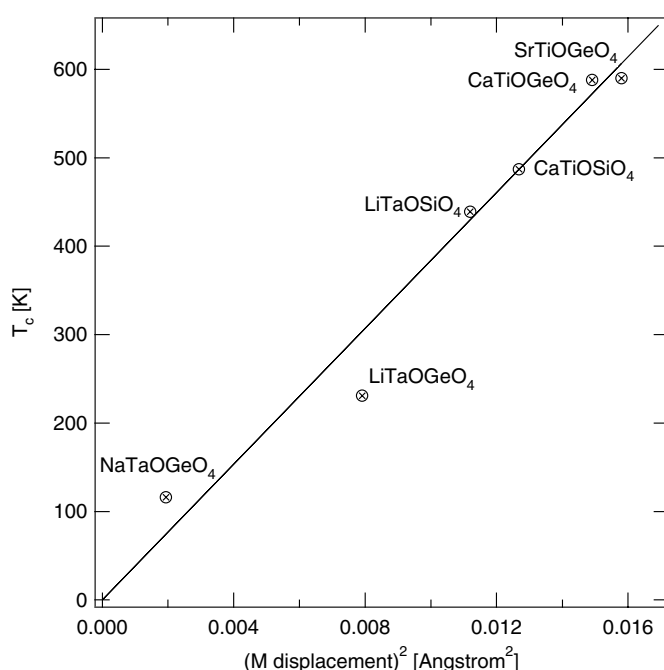


**Figure 2.** Critical temperature as a function of squared M-cation displacement in various compounds of the titanite structure type. Structure data and critical temperatures have been obtained from Kek *et al* (1997) (titanite), Malcherek (2002) (LiTaOGeO<sub>4</sub>), Genkina and Mill (1992) and Malcherek *et al* (2004) (LiTaOSiO<sub>4</sub>), Ellemann-Olesen and Malcherek (2005a) (CaTiOGeO<sub>4</sub>) and Ellemann-Olesen and Malcherek (2005b) (SrTiOGeO<sub>4</sub>). Details of the phase transition in NaTaOGeO<sub>4</sub> will be published elsewhere.

ranging from  $P\bar{1}$  to  $C2/c$ . However, only those compounds in which M is an early transition metal appear to occur in the distorted and ordered form of  $P2_1/c$  symmetry.

The chemically pure form of the mineral titanite undergoes a structural phase transition from the titanite aristotype structure of space group symmetry  $C2/c$  to  $P2_1/c$ , indicated by the appearance of sharp Bragg reflections at the  $h + k = \text{odd}$  positions of reciprocal space on crossing  $T_c$  from higher temperatures (Taylor and Brown 1976)<sup>1</sup>. In its low temperature form ( $P2_1/c$ ) titanite exhibits an ordered sequence of short and long Ti–O bonds. Coupled to this Ti displacement is a smaller Ca displacement. The transition occurs at a critical temperature of about 490 K in titanite. In contrast to the perovskite ferroelectrics the transition is of the zone-boundary type. The low temperature form might best be described as antipolar (Lines and Glass 1977) or as ‘hard antiferroelectric’ (Zhang *et al* 1995). Consequently the Ti displacements are antiparallel with respect to neighbouring chains. Figure 2 presents an overview of critical temperatures for all occurrences of the  $P2_1/c \leftrightarrow C2/c$  transition known to date.  $T_c$  is plotted as a function of the squared displacement of the transition metal cation M from its special position in the titanite aristotype structure. To obtain this static displacement, structure data for the lowest available measurement temperatures have been used for each compound. In the case of NaTaOGeO<sub>4</sub> this temperature is  $0.845 T_c$  and the order parameter might not be fully saturated. This might explain why the associated point in figure 2 plots slightly to the left of the

<sup>1</sup> Taylor and Brown (1976) reported the symmetry change using the non-standard space group settings  $P2_1/a$  and  $A2/a$ . Here a different setting based on the  $C2/c$  space group with the octahedral chains parallel to [001] is used instead.

obtained line. A linear relationship  $k_B T_c = K(\Delta z)^2/2$ , where  $k_B$  is the Boltzmann constant,  $\Delta z$  is the static displacement of the homopolar atom and  $K$  has the dimensions of a force constant, has been established by Abrahams *et al* (1968) for certain ferroelectrics. In another form the relationship can be expressed with  $(\Delta z)^2$  replaced by the square of the saturation polarization,  $P^2(T = 0)$ . In the present case the polarization is replaced by a sublattice polarization, as we are dealing with a set of centrosymmetric and therefore non-ferroelectric compounds. The AKJ relation essentially follows from the soft-mode picture of displacive phase transitions, as the energy stored in the distorted phase at low temperatures has to equal the thermal energy at the critical temperature (cf also Kozlov *et al* 1983).

The first observation of diffuse scattering intensity at the critical zone boundary position of natural titanite samples dates back to the first refinement of the stable, ambient temperature structure by Speer and Gibbs (1976). Higgins and Ribbe (1976) reported the occurrence of planes of diffuse scattering intensity normal to the octahedral chain direction in natural titanite samples. In natural samples Fe or Al often partially substitute for Ti, charge balanced by  $\text{OH}^-$  or  $\text{F}^-$  (Taylor and Brown 1976). The defects suppress the complete transition to the ordered  $P2_1/c$  form, as they stabilize domain walls that separate antiphase domains with an opposite sense of Ti displacement. These domains are essentially cylindrical, with their axes pointing parallel to the octahedral chain direction. Many studies aimed at the composition and temperature control of these diffuse scattering effects and the related domain structure have been conducted (Hollabaugh and Foit Jr 1984, Van Heurck *et al* 1991, Chrosch *et al* 1997, Kek *et al* 1997, Malcherek *et al* 2001). At  $T_c$  Bragg reflections, indicative of the transition to the  $P2_1/c$  phase, appear on top of a diffuse scattering background that extends in layers normal to [001]. Moreover, just above  $T_c$  a further diffuse scattering component localized at the position of the critical zone boundary position precedes the appearance of the Bragg maxima. The total diffuse scattering intensity diverges at  $T_c$  (Malcherek *et al* 2001).

In titanite the diffuse scattering disappears above roughly 850 K (Kek *et al* 1997). Several excess properties indicate the existence of an intermediate phase above  $T_c$  and below  $T_i \approx 825$  K (e.g. Salje *et al* 1993, Zhang *et al* 1997, Malcherek 2001). It is assumed that only for  $T > T_i$  is Ti truly located at the symmetry centre, with Ca at the 4e position of space group  $C2/c$ . This is also indicated by high pressure experiments at non-ambient temperatures (Kunz *et al* 2000). In the intermediate temperature region a split Ca position (Kek *et al* 1997) is observed and local off-centre Ti shifts probably occur as well (Malcherek *et al* 2001). The appearance of a similar intermediate phase has been confirmed for several isostructural phases of titanite (e.g. Malcherek *et al* 2004, Ellemann-Olesen and Malcherek 2005a).

In the titanite structure individual octahedral chains are isolated from one another. Therefore it is not surprising that displacement correlations occur in one dimension only, giving rise to just a single set of diffuse scattering rellanes. With the exception of  $\text{LiTaOSiO}_4$  and  $\text{SrTiOGeO}_4$  (powder diffraction data only) similar sheets of diffuse scattering have been found at temperatures above  $T_c$  in all of the compounds shown in figure 2. Anisotropic diffuse scattering in  $\text{LiTaOGeO}_4$  at ambient temperature is demonstrated in figure 3. In this compound the order–disorder component of the  $P2_1/c \leftrightarrow C2/c$  transition has been indirectly observed, as the  $^7\text{Li}$  MAS NMR spectra do not change across the phase transition. Determination of the quadrupolar coupling constant by computational *ab initio* methods indicates that a clear change of the spectra should be observable if the transition were of the purely displacive type, with Li occupying the 4e position in the  $C2/c$  phase (Malcherek *et al* 2004). The observation of a bimodal Li position at ambient temperature (Malcherek 2002), with Li remaining in a distorted tetrahedral coordination through the phase transition, is in agreement with these findings.

In an attempt to model the diffuse scattering observed in titanite, Malcherek *et al* (2001) assumed a static, uniform displacement of all Ti within individual octahedral chains. The

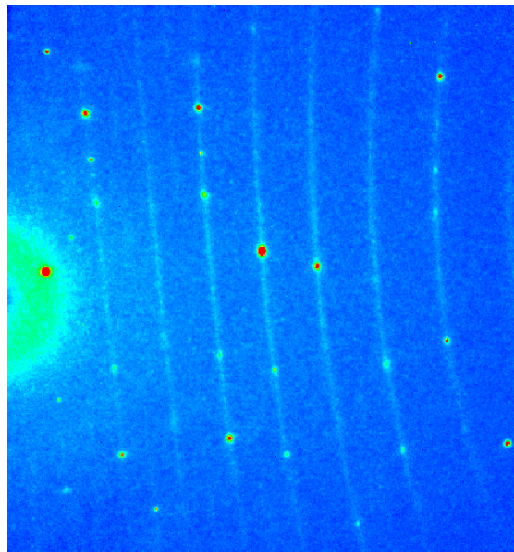


**Figure 3.** Diffraction image showing the intersection of diffuse scattering sheets on reciprocal planes  $(0, 0, l = 2n)$  in  $\text{LiTaOGeO}_4$  at ambient temperature ( $T = 1.29T_c$ ). Data were collected at beamline F1 of HASYLAB/DESY with  $\lambda = 0.4 \text{ \AA}$  radiation.  $[001]$  points approximately from left to right.

displaced position of the Ti atom was obtained from the distorted low temperature phase, while the coupled Ca displacements have been neglected. The one-dimensional displacement pattern is tantamount to a pseudo-spin model on a two-dimensional lattice, with each lattice point representing the displacement value (up or down) within a particular octahedral chain. For a completely random configuration of chain displacements a uniform diffuse scattering sheet normal to the chain direction has been obtained by Fourier transformation, as expected. In order to introduce inter-chain correlations of the displacements, configurations of the spin-1/2 Ising model at suitable temperatures were obtained by Monte Carlo simulation and then mapped to corresponding displacement configurations of the titanite structure. Fourier transformation rendered the simulated diffuse scattering in good agreement with the observed diffuse scattering intensity distribution (Malcherek *et al* 2001).

### 3. Pyrochlore type structures

A common oxide structure involving a three-dimensional framework of corner-connected oxygen octahedra is the cubic pyrochlore structure for stoichiometries  $\text{A}_2\text{B}_2\text{O}_7$ . The structure can be thought of as being built from two intertwined networks, one being formed by corner-sharing  $\text{BO}_6$  octahedra and the other consisting of O–A–O-bonds that form a cuprite like framework. Seen down one of the  $\langle 110 \rangle$  directions (figure 4), the structure appears to consist of crossing chains of  $\text{BO}_6$  octahedra and parallel O–Cd–O zigzag chains. Each octahedron shares all corner oxygens with adjacent octahedra, but trans-connections with respect to the B atom only occur along  $\langle 110 \rangle$ . Consequently linear chains of octahedra do not cross at  $90^\circ$  angles as in the cubic perovskites, but at  $60^\circ$  angles.

Among the compounds with the pyrochlore structure  $\text{Cd}_2\text{Nb}_2\text{O}_7$  (CNO) and  $\text{Cd}_2\text{Re}_2\text{O}_7$  (CRO) have attracted most interest in recent years. CRO has been identified as an oxide superconductor (Hanawa *et al* 2001, Sergienko *et al* 2004). CNO is known for its unusual

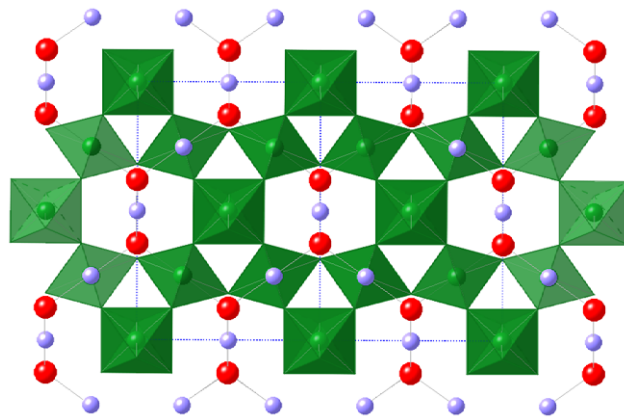


**Figure 4.** The structure of  $\text{Cd}_2\text{Nb}_2\text{O}_7$  viewed down one of the  $\langle 110 \rangle$  directions.

ferroelectric properties (Tachibana *et al* 2004), showing all the typical features of relaxor materials without the customary compositional disorder. However, surprisingly few single crystal diffraction studies of CNO have been published so far, even though many articles have been devoted to the ferroelectric properties of CNO (e.g. Kolpakova *et al* 1994, Ang and Yu 2004). CNO has cubic space group symmetry  $Fd\bar{3}m$  above  $T_S = 204$  K. At and below  $T_S$  several structural phase transitions occur Buixaderas *et al* (2001) and Tachibana *et al* (2004). According to Buixaderas *et al* (2001) the phase transition at  $T_S$  is improper ferroelastic while a proper ferroelectric transition occurs at  $T_c = 196$  K. However, many open questions remain regarding the symmetry and unit cell of the ferroelastic phase, the origin of the relaxor behaviour and the character of further structural phase transitions at lower temperatures.

A single crystal fragment of CNO was measured at HASYLAB beamline F1 at DESY/Hamburg using a MARCCD 165 detector. As the reconstructed reciprocal space map of the  $h1l$ -layer demonstrates (figure 5), diffuse scattering planes extend perpendicular to the  $\langle 110 \rangle$  directions of the cubic paraphase. The reciprocal space reconstruction was carried out using a set of programs developed by the author.

#### 4. Discussion

Because chain-like correlations similar to those in the perovskite structures are necessarily guided by the one-dimensional chain topology in the titanite structure, interpretation of the resulting diffuse scattering effects in the titanites is simpler. There is as yet no direct spectroscopic evidence for local displacements of the transition metal cation in the titanite paraphase. However, given the fact that the displacement of the M cation is the driving order parameter of the  $P2_1/c \leftrightarrow C2/c$  transition, it is reasonable to assume that such local displacements do exist. This is also indicated by the good agreement of the static model of Malcherek *et al* (2001) with the observed diffuse scattering. Unlike in titanite itself, the macroscopic displacement of the M cation in the low temperature phase is not always entirely directed towards the chain-forming O1 atom. For example, the Ta displacement in  $\text{LiTaOGeO}_4$  does have a rather large component off the Ta–O1 bond direction of the high temperature phase (Malcherek 2002). The correlations that give rise to the diffuse scattering sheets have to occur along a kinked chain of M–O–bonds, with the average M–O–M-angle being approximately given by the bond angle M–O1–M of the  $P2_1/c$ -ordered structure. This



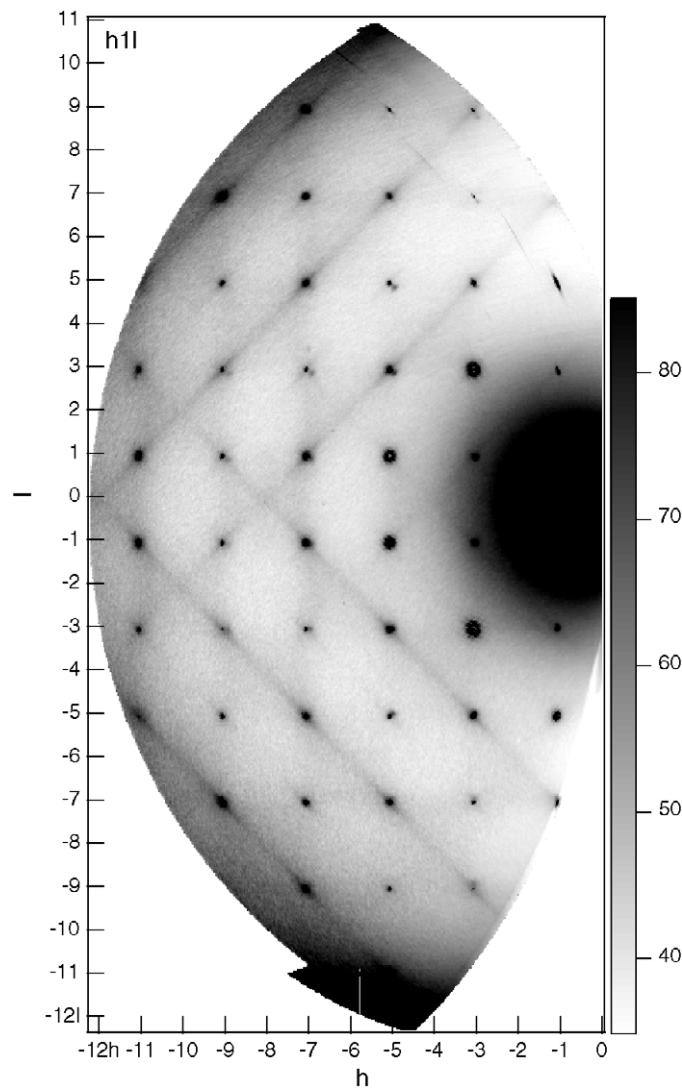


**Figure 5.** Reconstructed reciprocal space mapping of the  $(h1l)$  layer of CNO. Diffuse intensity planes normal to  $(110)$  that cut the reconstructed layer at an angle of  $90^\circ$  are clearly visible. Relplanes that intersect the layer at  $45^\circ$  appear broader and are therefore just barely recognizable.

angle ranges between  $140^\circ$  and  $150^\circ$  for the known titanite structures. In the ferroelectric perovskites the corresponding angle has more variability due to the eight-site disorder, but on average it can be expected to be smaller than  $180^\circ$  as well. By analogy to the perovskite structures, the nanodomains to be expected in the intermediate phase of the titanites are all parallel and cylindrical. The diameter diminishes with increasing temperature, as the lateral correlation of the Ti displacements is lost. The dynamics are limited to switching between the two displacement directions. The average length of these nanodomains has been estimated to be of the order of  $200 \text{ \AA}$  from the width of the diffuse scattering (Malcherek *et al* 2001) and of the order of  $60 \text{ \AA}$  from thermodynamic considerations (Hayward *et al* 2000). For the perovskite ferroelectrics Comes *et al* (1968) give an estimated chain length of  $50\text{--}100 \text{ \AA}$ .

In  $\text{Cd}_2\text{Nb}_2\text{O}_7$  chains of trans-corner-sharing  $\text{NbO}_6$  octahedra are oriented normal to the observed diffuse scattering sheets. It is therefore tempting to assume correlation of off-centre Nb displacements as the cause of this diffuse scattering, by analogy to the other compounds. Work to further examine this possibility is currently under way.

## 5. Conclusions

The above examples demonstrate the widespread occurrence of anisotropic diffuse scattering effects in early transition metal oxide structures. The dependence of the diffuse scattering on temperature, pressure or composition may provide valuable insights into the mechanisms and driving forces of structural phase transitions in such compounds, especially if other, more easily accessible, properties such as unit cell deformation are too small to be detected. As the example of CNO demonstrates, such diffuse scattering effects may have gone undetected even in well known materials.

## Acknowledgments

Synchrotron diffraction data reported here were obtained at beamline F1 of HASYLAB/DESY. The author is indebted to C Paulmann and U Bismayer for their support regarding these measurements. The author also wishes to thank I Glass for the synthesis of the CNO crystals. Financial support has been provided by the Deutsche Forschungsgemeinschaft.

## References

- Abrahams S C, Kurtz S K and Jamieson P B 1968 *Phys. Rev.* **172** 551–3  
Ang C and Yu Z 2004 *Phys. Rev. B* **70** 134103  
Bersuker I B 1966 *Phys. Lett.* **20** 589–90  
Brown I D 2002 *The Chemical Bond in Inorganic Chemistry* (Oxford: Oxford University Press)  
Buixaderas E, Kamba S, Petzelt J, Savinov M and Kolpakova N N 2001 *Eur. Phys. J. B* **19** 9–16  
Chapman B D, Stern E A, Han S, Cross J O, Seidler G T, Gavrilychenko V, Vedrinskii R V and Kraizman V L 2005 *Phys. Rev. B* **71** 020102  
Chaves A S, Barreto F C S, Nogueira R A and Zēks B 1976 *Phys. Rev. B* **13** 207–12  
Chrosch J, Bismayer U and Salje E 1997 *Am. Mineral.* **82** 677–81  
Comès R, Lambert M and Guinier A 1968 *Solid State Commun.* **6** 715–9  
Comès R, Lambert M and Guinier A 1970 *Acta Crystallogr. A* **26** 244–54  
Comès R and Shirane G 1972 *Phys. Rev. B* **5** 1886–91  
Denoyer F, Comès R and Lambert M 1971 *Acta Crystallogr. A* **27** 414–20  
Ellemann-Olesen R and Malcherek T 2005a *Am. Mineral.* **90** 1325–34  
Ellemann-Olesen R and Malcherek T 2005b *Phys. Chem. Minerals* **32** 531–45  
Genkina E A and Mill B V 1992 *Sov. Phys.—Crystallogr.* **37** 769–72  
Girshberg Y and Yacoby Y 1997 *Solid State Commun.* **103** 425–30  
Girshberg Y and Yacoby Y 1999 *J. Phys.: Condens. Matter* **11** 9807–22  
Hanawa M, Muraoka Y, Tayama T, Sakakibara T, Yamaura J and Hiroi Z 2001 *Phys. Rev. Lett.* **87** 187001  
Hayward S A, del Cerro J and Salje E K H 2000 *Am. Mineral.* **85** 557–62  
Higgins J and Ribbe P 1976 *Am. Mineral.* **61** 878–88  
Hollabaugh C and Foit F Jr 1984 *Am. Mineral.* **69** 725–32  
Hüller A 1969 *Solid State Commun.* **7** 589–91  
Kek S, Aroyo M, Bismayer U, Schmidt C, Eichhorn K and Krane H 1997 *Z. Kristallogr.* **212** 9–19  
Kolpakova N N, Margraf R and Polomska M 1994 *J. Phys.: Condens. Matter* **6** 2787–98  
Kozlov G V, Volkov A A, Scott J F, Feldkamp G E and Petzelt J 1983 *Phys. Rev. B* **28** 255–61  
Krakauer H, Yu R, Wang C, Rabe K M and Waghmare U V 1999 *J. Phys.: Condens. Matter* **11** 3779–87  
Kunz M, Arlt T and Stolz J 2000 *Am. Mineral.* **85** 1465–73  
Kunz M and Brown I D 1995 *J. Solid State Chem.* **115** 395–406

- Lines M E and Glass A M 1977 *Principles and Applications of Ferroelectrics and Related Materials* (Oxford: Clarendon)
- Malcherek T 2001 *Mineral. Mag.* **65** 709–15
- Malcherek T 2002 *Acta Crystallogr. B* **58** 607–12
- Malcherek T, Bosenick A, Cemič L, Fechtelkord M and Guttzeit A 2004 *J. Solid State Chem.* **177** 3254–62
- Malcherek T, Paulmann C, Domeneghetti M C and Bismayer U 2001 *J. Appl. Crystallogr.* **34** 108–13
- Mathan N d, Prouzet E, Husson E and Dexpert H 1993 *J. Phys.: Condens. Matter* **5** 1261–70
- Rabe K M and Waghmare U V 1997 *Ferroelectrics* **194** 119–34
- Ravel B, Stern E A, Vedrinskii R I and Kraizman V 1998 *Ferroelectrics* **206/207** 407–30
- Salje E, Schmidt C and Bismayer U 1993 *Phys. Chem. Minerals* **19** 502–6
- Sergienko I A, Keppens V, McGuire M, Jin R, He J, Curnoe S H, Sales B C, Blaha P, Singh D J, Schwarz K and Mandrus D 2004 *Phys. Rev. Lett.* **92** 065501
- Sicron N, Ravel B, Yacoby Y, Stern E A, Dogan F and Rehr J J 1994 *Phys. Rev. B* **50** 13168–80
- Speer J and Gibbs G 1976 *Am. Mineral.* **61** 238–47
- Tachibana M, Kawaji H and Atake T 2004 *Phys. Rev. B* **70** 064103
- Taylor M and Brown G E 1976 *Am. Mineral.* **61** 435–47
- Van Heurck C, Van Tendeloo G, Ghose S and Amelinckx S 1991 *Phys. Chem. Minerals* **17** 604–10
- Yu R and Krakauer H 1995 *Phys. Rev. Lett.* **74** 4067–70
- Zalar B, Laguta V V and Blinc R 2003 *Phys. Rev. Lett.* **90** 037601
- Zalar B, Lebar A, Seliger J, Blinc R, Laguta V V and Itoh M 2005 *Phys. Rev. B* **71** 064107
- Zhang M, Salje E and Bismayer U 1997 *Am. Mineral.* **82** 30–5
- Zhang M, Salje E, Bismayer U, Unruh H, Wruck B and Schmidt C 1995 *Phys. Chem. Mineral.* **22** 41–9